DYNAMIC ANALYSIS OF ROTATING CURVED BEAM WITH A TIP MASS

J.-H. Park and J.-H. Kim

Department of Aerospace Engineering, College of Engineering, Kwanak-Gu, San 56-1, Seoul National University, Seoul, Korea, 151-742

The dynamic characteristics of a rotating curved beam are investigated. The equations of motion include all dynamic effects such as Coriolis force, centrifugal force and acceleration. The analysis of the rotating beam takes into account the coupling between rigid-body motion and elastic deformation, such that geometrically non-linear effects are included in the model. For dynamic analysis, the time responses for accelerating motion and torque-driven motion are calculated. The natural frequencies for curved beams of various radii of curvature are then calculated as the rotating speed increases. This study mainly discussed the effect of curvature that can change the characteristics of the beam. The effects of tip mass on the dynamic response of the beam are also studied.

© 1999 Academic Press

1. INTRODUCTION

Dynamic analyses of elastic structures are studied for use in various structures such as space structures, robotics and high-speed turbine blades. A rotating system is affected by coupling between the rotating motion and the elastic deflection. The effect cannot be ignored, and is important to the motion. There are thus many researches about this geometrically non-linear behavior. Although most of the studies deal with straight beam or plate, a few researchers have shown interest in curved beams that are useful in many structures. Simo and Vu-Quoc [1] proposed an approach that formulates the dynamic response of a flexible beam subjected to large overall motions relative to the inertial frame. This approach uses a finite strain rod theory that is capable of treating finite rotations, which result in much simpler structure of the resulting equations. But, excessive calculation is required for treating dynamics of beams with small deformation because the approach uses finite strain rod theory. Simo and Vu-Quoc [2] studied the role of non-linear structural theories in transient dynamics analysis of flexible structures. For a rotating plane beam, a set of linear partial differential equations of motion was derived from fully non-linear beam theory by consistent linearization. Meek and Liu [3] derived the dynamic model of a flexible Timoshenko beam with geometrical non-linearities subject to large overall motions by using the finite element method and multi-body system formulation. For geometrical

non-linearities, non-linear strain–displacement relation was used. Kane *et al.* [4] obtained a comprehensive theory for dealing with small vibrations of a general beam attached to a base. A new variable, namely the stretch in the beam along the elastic axis, is used to account for the geometric non-linearity appropriately. Fallahi and Lai [5] presented an improved numerical method with three new features. First, the time separation concept is introduced to allow time-independent terms to be computed separately and assembled with time-dependent terms in each time-marching cycle to form global system equations. Second, the Timoshenko beam with non-linear geometric stiffness is modelled with exact tangent matrix as opposed to conventional pseudo-tangent matrix approximation. Third, the computational scheme is implemented in homogeneous co-ordinates that provide a more natural and efficient vector representation. The computing time is thus reduced by more than 70% compared to the work of Fallahi and Lai [4]. Haering *et al.* [6] used the same approach as in reference [4] and suggested the augmented imbedded geometric constraint approach. It allows the solution of problems in the case the lateral deflection of the beam is dominated by either bending or membrane stiffness. Iura and Atluri [7] presented an efficient formulation in which both an inertial frame and a rotating frame are introduced to simplify computational manipulation. The kinetic energy of the system is obtained by using the inertial frame and the rotating frame together with the small strain assumption to derive the strain energy of the system. Inna Sharf [8] explained and compared the different approaches that had been developed for geometric stiffening through an in-depth review of several publications. The review offers an understanding of the existing methods and how they relate to one another. The authors and references mentioned above are all concerned with the geometric stiffening effect. The objects that have been treated, however, are straight beams and plates. The first part of this research deals with the transient motion of a curved beam which is useful in many complicated structures, and compare the results with the behavior of a straight beam.

For investigating the characteristics of a curved beam from a different perspective, it is helpful that we observe how the natural frequency varies. The following references deal with the natural frequency of straight beams and explain the characteristics. Yamaura and Ono [9] analyzed the dynamic behavior of the beam driven by torque. Formulation considering geometrical non-linearity was used. They also verified the exactness of the formulation by conducting experiments. Shabana and Schwetassek [10] demonstrated the equivalence of two conceptually different formulations used in flexible body dynamics. These two formulations are the floating frame of reference approach, and the absolute nodal co-ordinate formulations. Chen and Mucino [11] compared the difference between the linear model and the non-linear model when prescribed torque drives a beam. Putter and Manor [12] calculated the eigenvalues and mode shapes of the rotating beam with a constant speed. This research indicates that the eigenvalues increase as the rotating speed increases. Yigit *et al.* [13] derived the equations of motion of the rotating beam which does not use non-linear strain–displacement relationship, but a centrifugal energy. The studies of curved beam have been mostly about static analysis, and the dynamic characteristics of the beam with initial imperfection or

small curvature have been investigated. There is, however, a special behavior of the rotating curved beam when the curvature is somewhat large. The research of curved beam with moderate curvature will thus be important for understanding the characteristics of the curved structures. Krishnan and Suresh [14] investigated the effect of shear deformation on deflection and shear deformation together with rotary inertia on natural frequencies of the curved beam using a simple cubic linear beam element. Stolarski and Beytschko [15] explained the membrane locking. This effect can appear when low order, in-plane displacements are used. Reduced integration eliminates membrane locking. Wang and Mahrenholtz [16] performed the dynamic analysis of the rotating curved beam that has the curvature in both in-plane direction and out-of-plane direction. But, only small radii of curvature are considered. This study shows that natural frequency also increases as the rotating speed increases. The result is the same as the behavior of a straight beam. Hodges *et al.* [17] suggested numerical solution based on finite element method of an initially curved and twisted beam.

This study focuses on two aspects. The dynamic motion of a curved beam is computed first for a prescribed rotation angle and a torque. The study reveals the characteristics of a curved beam that are different from a straight beam. Secondly, the natural frequencies are calculated for various rotating speeds. The natural frequencies of a curved beam show a different trend from that of a straight beam. First, the non-linear strain–displacement relationship is applied to obtain strain energy [5]. Second, the consistent linear equations of motion are derived for efficient calculation [2]. The finite element method is used for the numerical method. The Newmark time integration and Newton–Raphson iteration methods are used for solving the non-linear equations of motion.

2. THEORY

Figure 1 shows the model of the curved beam. The beam is idealized as a cantilever with a tip mass at the end. Only the motions in the plane are considered in this study, and the shear deformation and the rotary inertia are considered within the formulation.

The rotating beam has a coupling between the lateral deformation and the rigid body motion. The centrifugal force affects the lateral displacement after the beam is deformed even if the deformation is very small. However, the strain energy obtained by using the linear strain–displacement relationship cannot appropriately account for this stiffening effect. There are mainly three methods for considering this geometric non-linearity. First, the non-linear strain–displacement relationship is used for deriving the strain energy [3, 4, 7]. Second, a new variable, the stretch in the beam along the elastic axis, is introduced instead of the variable, to represent the displacement along the elastic axis. This method can make the strain energy linear but the inertia terms complicated [5, 6]. The method is eventually the same as the first method [2]. Third, the consistent linear equations can be derived for the small deformation assumption. It considers the centrifugal forces as the potential energy after the deformation occurs [2]. In this study, non-linear
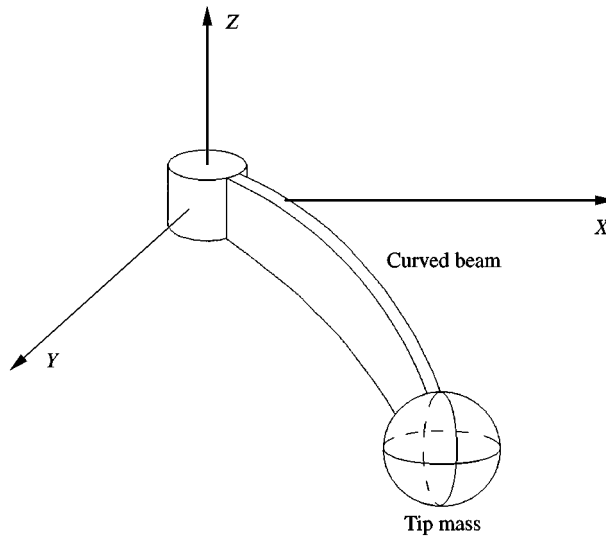
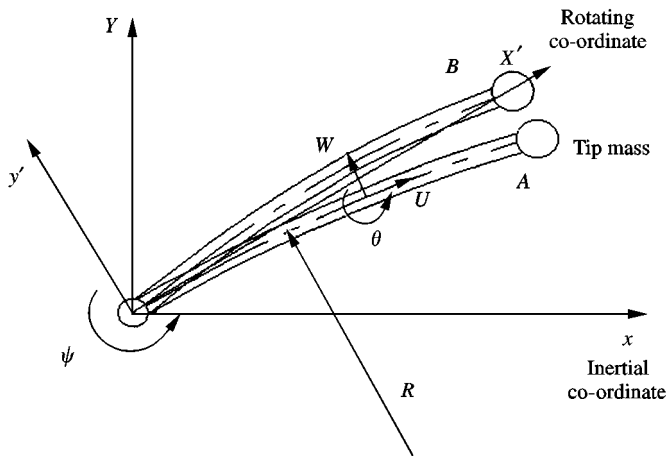Figure 1. Model of the curved beam.

Figure 2. Geometry of the rotating curved beam.

strain–displacement relationship accounts for the coupling effect, and then a consistent linear formulation is proposed for the small deformation.

2.1. THE DISPLACEMENT FIELD AND THE STRAIN–DISPLACEMENT RELATIONSHIP

Figure 2 shows the curved beam model considering the shear effect. The displacement fields are as follows:

$$u_1(x, y, t) = u(x, t) - y\theta(x, t),$$
$$u_2(x, y, t) = w(x, t),$$

(1)

where x denotes the position along the neutral axis from the left end and y denotes the position along the normal (thickness direction) to the neutral axis at the position x. u and w represent the displacements in the x and y directions respectively. θ represents the rotation angle of the normal to the neutral axis.

The non-linear strain–displacement relationship equations are [18]

$$\varepsilon_{xx} = \frac{1}{\alpha}\frac{\partial u_1}{\partial x} + \frac{u_2}{\alpha}\frac{\partial \alpha}{\partial y} + \frac{1}{2}\left(\frac{1}{\alpha}\frac{\partial u_2}{\partial x}\right)^2, \tag{2}$$

$$\gamma_{xy} = \frac{1}{\alpha}\frac{\partial u_2}{\partial x} + \frac{\partial u_1}{\partial y} - \frac{u_1}{\alpha}\frac{\partial \alpha}{\partial y}, \tag{3}$$

where $\alpha = (R + y)/R$.

The third term of equation (2) represents the non-linearity and account for the coupling effect with the first term.

2.2. THE KINETIC ENERGY

The position vector in the local co-ordinate system can be expressed as follows (Figure 2):

$$X^{local} = \begin{bmatrix} (R+y)\sin\left(\dfrac{x}{R}\right) \\ -(R+y)\left(1 - \cos\left(\dfrac{x}{R}\right)\right) \end{bmatrix} + \begin{bmatrix} \cos\left(\dfrac{x}{R}\right), & \sin\left(\dfrac{x}{R}\right) \\ -\sin\left(\dfrac{x}{R}\right), & \cos\left(\dfrac{x}{R}\right) \end{bmatrix} \begin{Bmatrix} u \\ w \end{Bmatrix} \equiv X + \Phi U. \tag{4}$$

We define the rotation of the rotating co-ordinate system about the inertia co-ordinate as ψ. Then, the rotation matrix and the position vector in the inertia co-ordinates are expressed as follows:

$$\Psi = \begin{bmatrix} \cos\psi, & \sin\psi \\ -\sin\psi, & \cos\psi \end{bmatrix}, \quad X^{global} = \Psi X^{local} = \Psi(X + \Phi U), \tag{5}$$

$$T = \frac{1}{2}\int_v \rho |\dot{X}^{global}|^2 \, \mathrm{d}v$$

$$= \frac{1}{2}\int_v \rho \{\dot{\psi}^2(U^{\mathrm{T}}\Phi^{\mathrm{T}}\Phi U + 2X^{\mathrm{T}}\Phi U + X^{\mathrm{T}}X)$$

$$+ 2\dot{\psi}(X^{\mathrm{T}}J\Phi\dot{U} + U^{\mathrm{T}}\Phi^{\mathrm{T}}J\Phi\dot{U} + \dot{U}^{\mathrm{T}}\Phi^{\mathrm{T}}\Phi\dot{U}\} \, \mathrm{d}v, \tag{6}$$

where ρ is the density of the material and

$$J = \begin{bmatrix} 0 & 1 \\ -1 & 0 \end{bmatrix}.$$

The displacement field equation (1) can be transformed into a matrix form

$$\begin{Bmatrix} u_1 \\ u_2 \end{Bmatrix} = \begin{pmatrix} 1 & 0 & -y \\ 0 & 1 & 0 \end{pmatrix} \begin{Bmatrix} u \\ w \\ \theta \end{Bmatrix} \equiv Nq.$$

The kinetic energy is expressed as

$$T = \frac{1}{2} \int_v \rho \{ \dot{\psi}^2 (q^T N^T \Phi^T \Phi N q + 2X^T \Phi N q + X^T X)$$

$$+ 2\dot{\psi}((X^T J \Phi N \dot{q}) + N^T q^T \Phi^T J \Phi N \dot{q}) + \dot{N}^T q^T \Phi^T \Phi N \dot{q} \} \, dv. \quad (7)$$

2.3. THE EQUATIONS OF MOTION

When the rotation angle ψ is prescribed, the non-linear equations of motion can be expressed using Hamilton's principle as follows:

$$\mathbf{M}\ddot{q} + \mathbf{C}\dot{q} + (\mathbf{G} + \mathbf{K})q + \mathbf{P}(q) + \mathbf{F} = \mathbf{0}, \quad (8)$$

where

$$\mathbf{M} = \int_A N^T \Phi^T \Phi N \, dA, \quad \mathbf{C} = \dot{\psi} \int_A N^T \Phi^T (J^T - J) \Phi N \, dA,$$

$$\mathbf{G} = \ddot{\psi} \int_A N^T \Phi^T J^T \Phi N \, dA - \dot{\psi}^2 \int_A N^T \Phi^T \Phi N \, dA,$$

$$\mathbf{F} = \ddot{\psi} \int_A N^T \Phi^T J^T X \, dA - \dot{\psi}^2 \int_A N^T \Phi^T X \, dA, \quad q = \{u_1, u_2, \theta\}^T.$$

The matrix $\mathbf{C}$ represents Coriolis effect, and the first terms of the matrices $\mathbf{G}$ and $\mathbf{F}$ represent the inertia force caused by the accelerating rotation. The second terms of the matrices $\mathbf{G}$ and $\mathbf{F}$ are the centrifugal forces. The matrix $\mathbf{K}$ represents the stiffness matrix derived by the linear strain energy. The matrix $\mathbf{P}$ denotes the geometric non-linear effect (see Figure 3).

If we suppose that the deformation is small and we modify the non-linear terms of the strain energy, the consistent linear equations of motion will be derived.
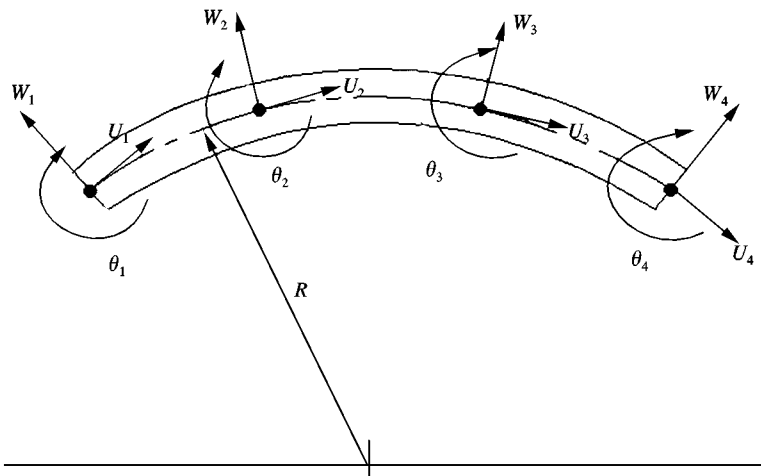

Figure 3. Element geometry and nodal degrees of freedom.

Equation (2) is divided into linear term ε_l and non-linear term ε_{non},

$$\varepsilon_{xx} = \varepsilon_l + \varepsilon_{non}. \tag{9}$$

The virtual work of ε_{xx} is

$$\delta U = \int E(\varepsilon_1 + \varepsilon_{non})(\delta\varepsilon_l + \delta\varepsilon_{non})\,\mathrm{d}v$$

$$\cong \int (E\varepsilon_l\delta\varepsilon_l + \tau_{xx}\delta\varepsilon_{non})\,\mathrm{d}v, \tag{10}$$

where τ_{xx} is the normal stress of the cross-section of the beam by the centrifugal force.

The normal stress τ_{xx} can be calculated as follows:

$$\tau_{xx} = \rho R^2\dot{\psi}^2\left\{1 - \cos\left(\frac{x}{R} - \frac{L}{R}\right) + \left(\frac{L}{R} - \frac{x}{R}\right)\sin\left(\frac{x}{R}\right)\right\}, \tag{11}$$

where R is the radius of curvature and $\dot{\psi}$ is the velocity of rotation.

Therefore, equation (8) can become the consistent linear equation

$$\mathbf{M}\ddot{q} + \mathbf{C}\dot{q} + (\mathbf{G} + \mathbf{K} + \mathbf{K}')q + \mathbf{F} = 0, \tag{12}$$

where $\mathbf{K}'$ denotes the effect of the centrifugal force on the lateral deflection and is proportional to the square of the rotation speed.

2.4. THE NATURAL FREQUENCY OF A CURVED BEAM ROTATING AT CONSTANT SPEED

The natural frequencies can be calculated through two models: non-linear and consistent linear model. Generally, the constantly rotating curved beam has a deformed shape, which should be considered [17]. For the non-linear model, the deformed shape must be calculated first and then the natural frequencies are obtained in the deformed state. However, for the consistent linear model, the linear eigenvalue problems are derived regardless of the deformed configuration because the equations are derived under the assumption that the deformations are small. Eventually, the method using the consistent linear model calculates the natural frequencies based on the original configuration. Since the focus is on small deformation in this study, the above-mentioned methods are applied to obtain the natural frequencies and the results are compared. To rewrite the equations in a dimensionless form, the length is non-dimensionalized by the total length L of the curved beam and the time is non-dimensionalized by $\sqrt{\rho A L^4/EI}$.

3. NUMERICAL RESULT

3.1. THE STATE OF ACCELERATION AND CONSTANT ROTATION

The Newmark method is applied to integrate the equations for analyzing the motion of the curved beam numerically and the Newton–Raphson iteration method is used to solve the non-linear equation at each time step. The result is

based essentially on the non-linear model. The beam is subjected to a spin-up maneuver by prescribing the angle of revolution $\psi(t)$ as follows [2]:

$$\psi = \begin{cases} \dfrac{\psi_0}{T_0}\left\{ t - \dfrac{T_0}{2\pi}\sin\left(\dfrac{2\pi t}{T_0}\right)\right\} & (0 \leqslant t \leqslant T_0), \\ \\ \psi_0 & (t \geqslant T_0), \end{cases} \tag{13}$$

where T_0 is the time when the constant rotation starts, ψ_0 is the constant rotation speed and t is the time.

This type of motion was proposed in reference [4] to demonstrate that the conventional approach based on linear beam theory may lead to grossly inaccurate results: instability of a physically stable system. Also, this motion can show the characteristics of motion in a transient phase and a constant revolution phase. In this study, the local co-ordinate is rotated so that the x-axis connects the top and the bottom of the curved beam to make the comparison with a straight beam easier. In Figure 2, B denotes the transformed local co-ordinate. Figure 4 shows that the time response of the curved beam approaches that of the straight beam when the radius of curvature is very large. The radii -of curvature are selected as 10^2 and 10^4. The material properties are identical to those employed in reference [4]. The curve of the radius of curvature 10^4 represents the case of the large radius of curvature and is almost identical to that of a straight beam. The result of $R = 10^2$ shows the dynamic characteristics of a typical curved beam in accelerated and constantly rotating states. In an accelerated state, the maximum deflection decreases according to the effect of the curvature compared to that of a straight beam. In a constantly rotating state, the tip deflection vibrates around a certain value above 0 whereas the tip deflection of the straight beam oscillates around 0. This is due to
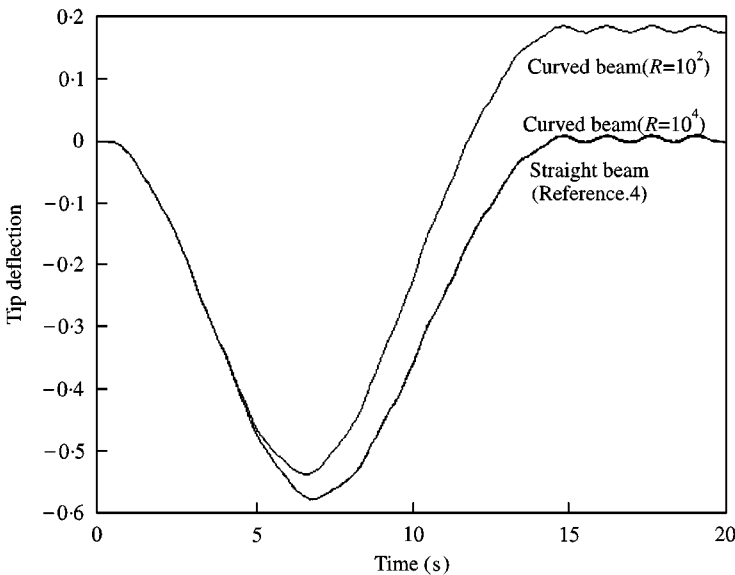

Figure 4. Dynamic response of the straight beam and the curved beam: $\psi 0 = 6$; $T0 = 15$; $\rho A = 1.2$; $\rho I = 6e - 4$; $EA = 2.8e7$; $EI = 1.4e4$; $GA = 1e7$; $L = 10$.

the difference of the centrifugal force between the curved beam and the straight beam. The formulation using linear beam theory may also lead to grossly inaccurate results in the curved beam case. So, the non-linear formulation must be applied to the curved beam. Figure 5 verifies this feature. The solution of the linear formulation shows the unreasonable motion of the tip deflection. However, the result of the non-linear theory is physically reasonable. The dynamic characteristics of the curved beam are investigated from two points of view; namely, a tip mass and curvature. The curved beam with a tip mass is analyzed in Figure 6. A tip mass is 0·2 times the total mass of the curved beam and we choose the amount as a typical value. The curve shows a physically reasonable result: a tip mass increases the amount of tip deflection in the accelerated state and lets the tip vibrate at smaller values than that of a straight beam in constantly rotating states. Figure 7 compares a non-linear model with a consistent linear model. When the radius of curvature is large, two models are indistinguishable. However, when the radius of curvature is sufficiently small, discrepancies are shown. This variance is obvious at the state of constant rotation.

3.2. THE MOTION OF THE CURVED BEAM DRIVEN BY TORQUE

The following torque drives the curved beam in the numerical analysis.

$$\tau = \begin{pmatrix} 80(0 \leqslant t < 5) \\ 0(5 \leqslant t < 10) \\ -80(10 \leqslant t < 15) \end{pmatrix}. \tag{14}$$
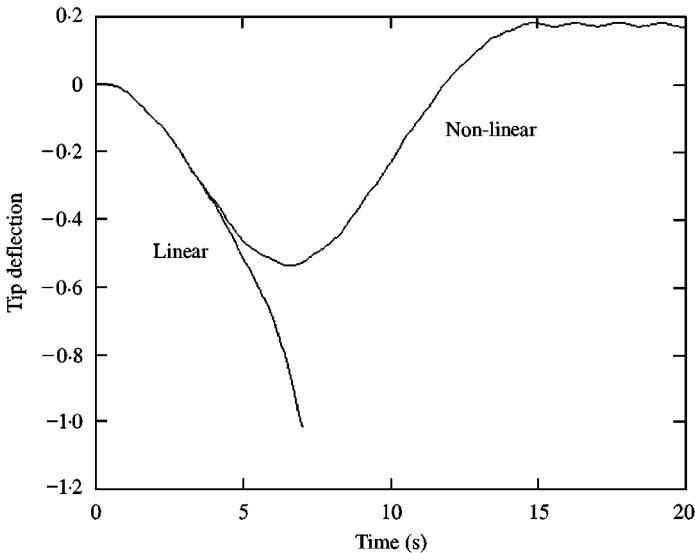

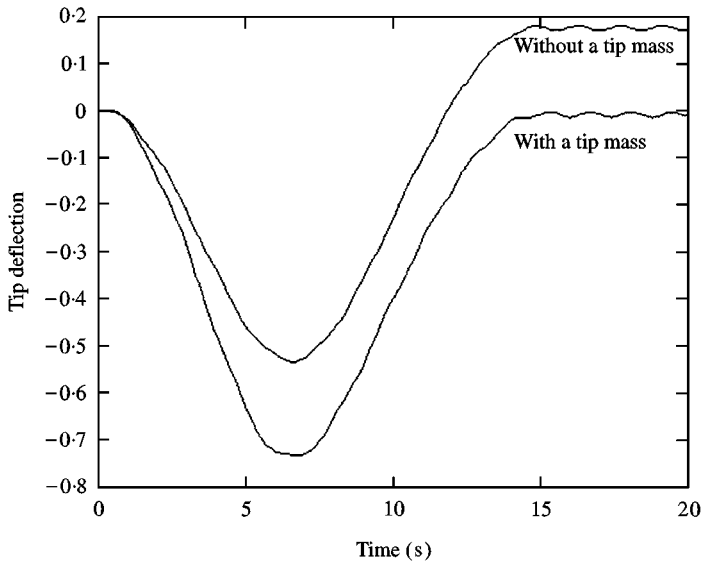Figure 5. Dynamic response of the linear model.

Figure 6. Dynamic response of the curved beam.

The non-linear equations are integrated by a Newmark time integration method. Solutions are obtained at each time step using the Newton–Raphson iteration method. Results are shown in Figure 8. The figures corresponding to $R = 100$ and 20 denote the illustrative cases of large and small radii of curvature respectively. The dotted curves are the results calculated by consistent linear formulations. The solid line curves are the solutions of non-linear formulations. The tip amplitude of the small radius of curvature is less than that of the large radius of curvature in vibration. The features are physically understandable when compared to the motions of the accelerated states. The tip deflection of the small radius of curvature is smaller than that of the large radius of curvature.

3.3. THE NATURAL FREQUENCIES OF THE CURVED BEAM

Some characteristics of the curved beam have been investigated by several previous analyses. Most of them mainly focus on the dynamic motions when the curved beam rotates by prescribed angle or by torque. In this section, natural frequencies are studied for deeper understanding. The analysis can be performed by identical methods: non-linear formulation and consistent linear method. The non-linear method will give more accurate results because it takes into account the deformed configuration. The only advantage of the consistent linear method is convenience in calculation and the resulting time saving. In the non-linear formulation, we have to obtain the deformed configuration at a certain rotating speed. The eigenvalues are then calculated by linearized equations at this deformed configuration. When using the consistent linear formulation, the eigenvalues are obtained just according to the rotating speed. This is why the consistent linear
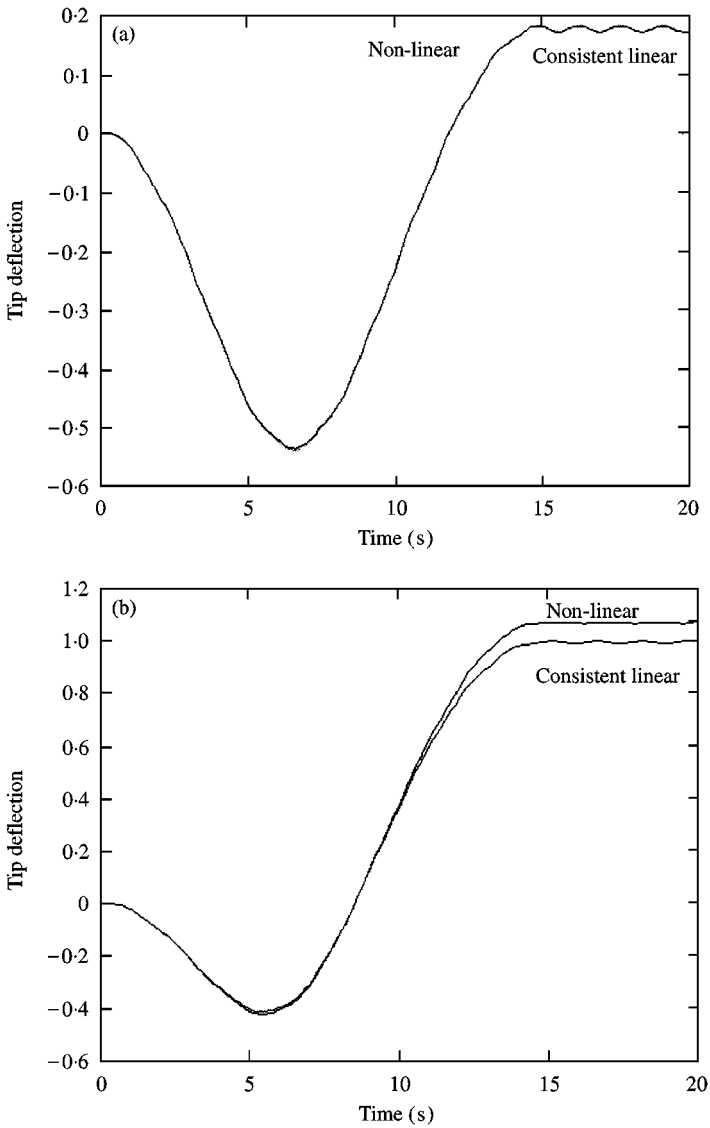
Figure 7. Comparison of the non-linear model and the consistent linear model. (a) Radius of curvature $R = 100$, (b) Radius of curvature $R = 20$.

formulation is assumed as the small deformation. The deformed configuration is not considered in the equations. The trends of the natural frequencies are examined first through the non-linear formulation, followed by the comparison of the two methods. The material properties of steel are used. The calculation of the natural frequencies does not contain the Coriolis force. The differences are below 4%.

3.3.1. *The natural frequencies of the various central angles*

The natural frequencies of the straight beam increase, as the rotating speed becomes large. In the case of the curved beam with a large radius of curvature,
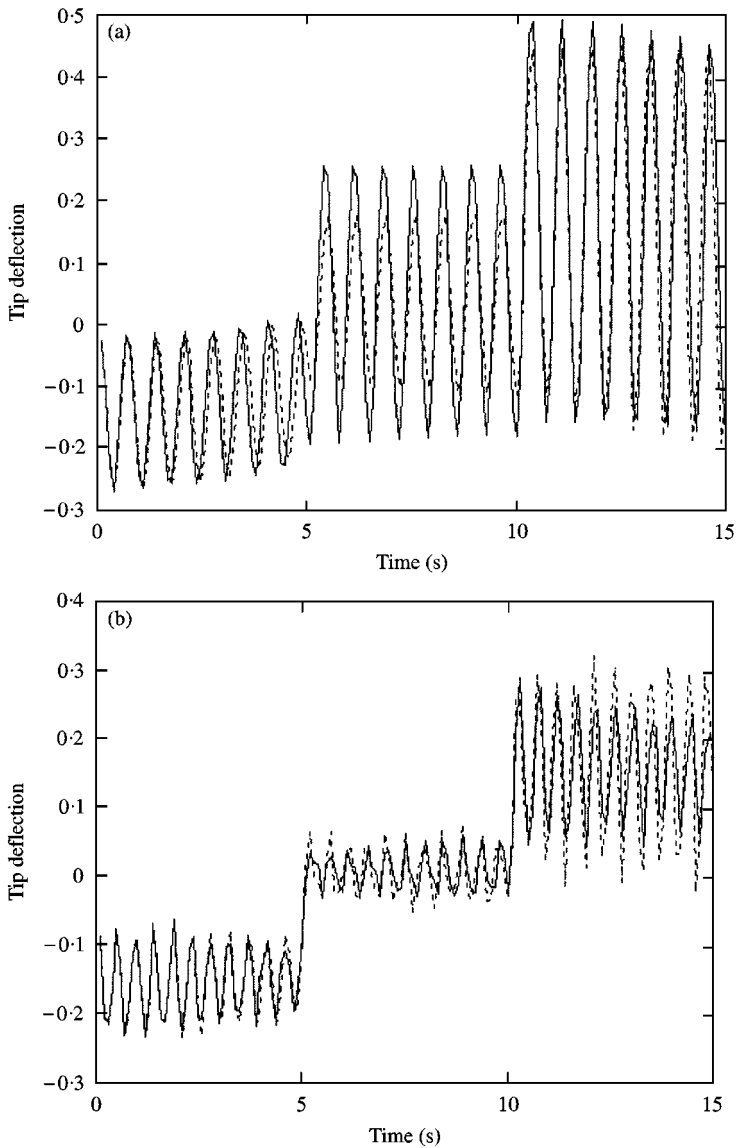
Figure 8. Torque driven motion of the curved beam: (a) Radius of curvature $R = 100$: (b) Radius of curvature $R = 20$: ------, consistent linear; ———, non-linear.

namely almost straight beam, the natural frequencies also increase like those of a straight beam. However, when a curved beam has a large curvature, the first natural frequency decreases. Generally, curved beams (arches) have been classified based on curvature in the following manner:

(1) shallow arch (subtended angle $< 40°$),
(2) moderately deep arch (subtended angle $= 40°$),
(3) deep arch ($40° <$ subtended angle $< 180°$),
(4) very deep arch (subtended angle $> 180°$).

When observing the trend of the natural frequencies according to this classification, we can say that the natural frequencies of shallow arch increase as the rotation speed increases. However, the first natural frequencies of deep arches decrease as the rotation speed increases while the other natural frequencies increase.

From Figures 9 and 10, the first natural frequencies of a non-linear beam model are plotted according to rotating speeds. The slenderness ratio is set as $R/t = 50$. The range of the central angle is from 10 to $90°$. The first natural frequencies of the beam without a tip mass are shown in Figure 9. In shallow arch beams, the natural frequencies increase as the rotating speed increases. But, the results of deep arch beams show the opposite behavior: the first natural frequencies decrease. Figure 10 shows the first natural frequencies of the curved beam with a tip mass. The curved beam with a tip mass is more deformed at the rotating state than the curved beam without a tip mass. The radius of curvature, thus becomes larger at the rotating state because of a tip mass. The enlarged radius of curvature renders higher natural frequencies. Although the extent of the effect depends on the amount of the tip mass, the subject will not be investigated further since only the main characteristics of curved beams are being considered here. The second natural frequencies are plotted in Figures 11–12. The same models are used for comparing the results. They all exhibit increasing trends as in the straight beam cases. In frequencies above the second natural frequencies, the trends are the same as the second natural frequencies.

3.3.2. *The comparison between the non-linear and the consistent linear formulation*

The consistent linear formulation is very effective when time simulation is performed and when the curvature is small. But, the calculated natural frequencies
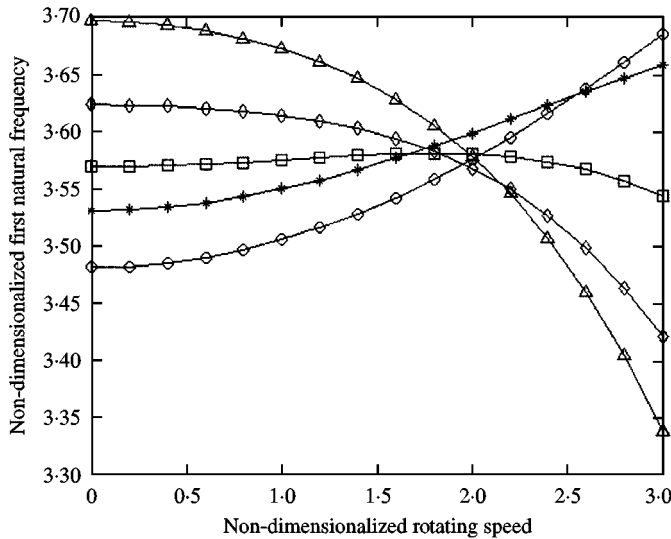

Figure 9. First natural frequency of the curved beam: ◇——◇, 10; ✳——✳, 30; □——□, 50; ◇——◇, 70; △——△, 90.
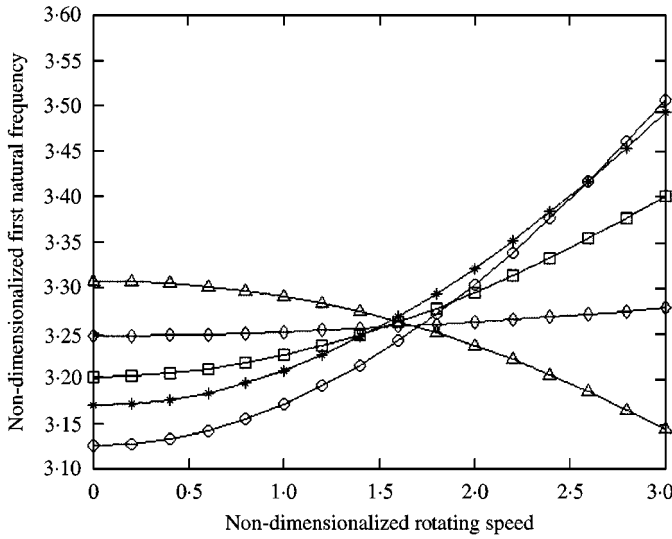
Figure 10. First natural frequency of the curved beam with a tip mass: ◇——◇, 10; ✶——✶, 30; □—□, 50; ◊——◊, 70; △—△, 90.
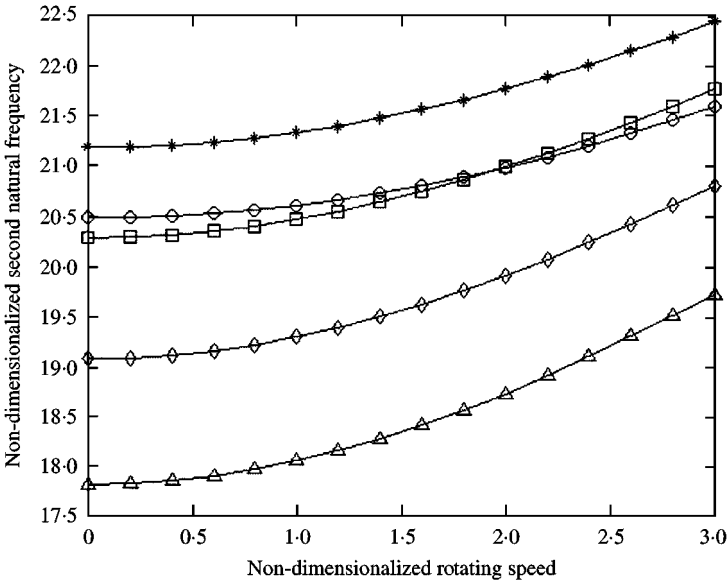
Figure 11. Second natural frequency of the curved beam: ✶——✶, 10; ◇——◇, 30; □—□, 50; ◊——◊, 70; △—△, 90.

are different from those of the non-linear formulation. These differences are investigated in Figures 13 and 14. For observation of the major characteristics, the central angles of 10, 50, 90° are selected. The dotted line and the solid line, respectively, denote the solutions of the consistent linear formulation and those of the non-linear formulation. In the case of the straight beam, the difference between two formulations is very small. The same trend occurs when the curved beam is
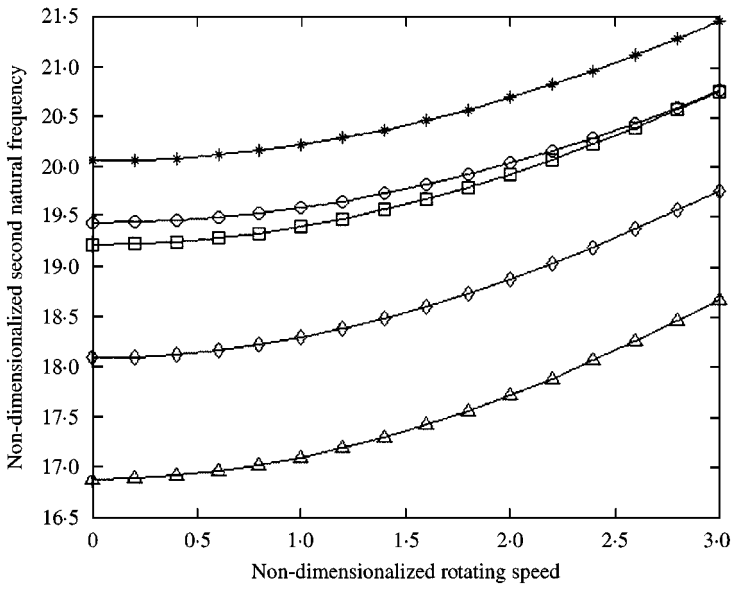
Figure 12. Second natural frequency of the curved beam with a tip mass: ✻——✻, 10; ◯——◯, 30; ☐—☐, 50; ◇——◇, 70; △—△, 90.
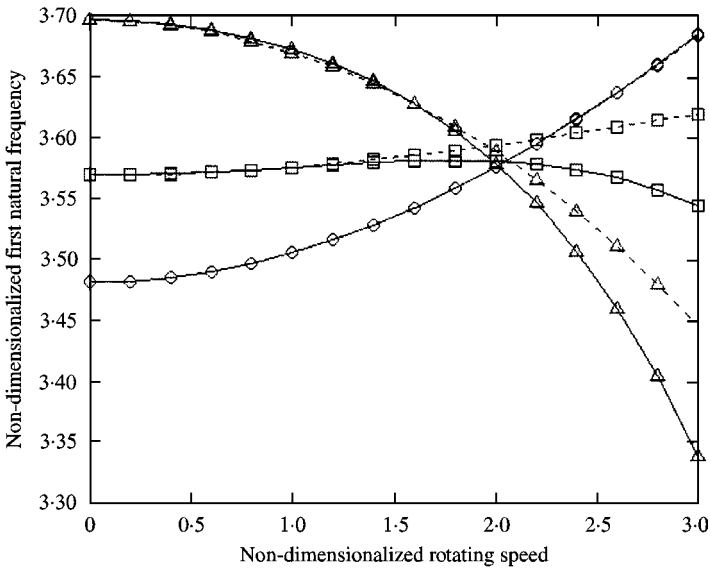

Figure 13. Comparison of the first natural frequency with non-linear and consistent linear model: ◯—◯, 10 non-linear; ◯--◯, 10 consistent linear; ☐—☐, 50 non-linear; ☐--☐, 50 consistent linear; △—△, 90 non-linear; △--△, 90 consistent linear.

bent little. The case of $10°$ in Figure 13 confirms this feature. However, the difference becomes large as the curvature increases. It is physically resonable. While the deformation is large at the big curvature, the consistent linear formulation cannot consider the deformed configuration. In other words, the consistent linear
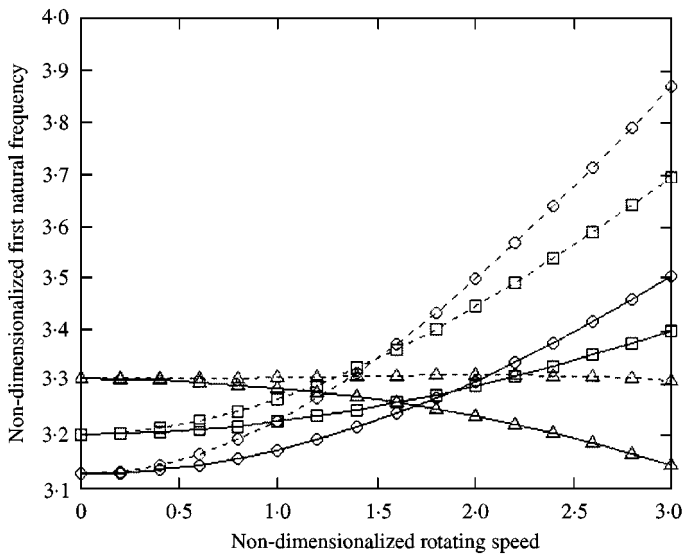
Figure 14. Comparison of the first natural frequency with non-linear and consistent linear model with a tip mass: O—O, 10 non-linear; O--O, 10 consistent linear; □—□, 50 non-linear; □--□, 50 consistent linear; △—△, 90 non-linear; △--△, 90 consistent linear.

formulation calculates the natural frequencies of the initial shape. The shape of the consistent linear formulation has more curved configuration than that of the non-linear formulation. Therefore, the natural frequencies of the consistent linear formulation have larger values than those of the non-linear formulation. The effects of a tip mass are shown in Figure 14.

4. CONCLUSION

The dynamic equations of motion that include the Coriolis effect, centrifugal forces, and accelerating forces are derived when a curved beam rotates. This study mainly investigated the characteristics of a curved beam compared to those of a straight beam. The effects of curvature and tip mass are also studied. This research is conducted through two procedures. First, the time simulations in accelerating and constantly rotating states are performed. The natural frequencies at the various rotating speeds are calculated based on the same two formulations. The different behaviors of curved beam depending on curvature and tip mass are summarized below.

1. The tip deflection of curved beam is less than that of a straight beam in the accelerated state.
2. A tip mass enlarges the tip deflection.
3. The tip amplitude of the small radius of curvature is less than that of the large radius of curvature in vibration.

Second, the natural frequencies are analyzed as the rotating speed increases. A straight beam's first natural frequency increases with the rotating speed, while

decreases in first natural frequency are observed for curved beams with a curvature over some certain value. However, the natural frequencies of curved beams with a tip mass increase as the rotating speed increases. The reason can be stated in two aspects: first, tip mass enlarges the centrifugal force. Second, the deformed shape has larger natural frequencies than the original configuration. The range within which the consistent linear model for the curved beam can be used is estimated by the calculated results.

REFERENCES

1. J. C. SIMO AND L. VU-QUOC 1986 *Journal of Applied Mechanics* **53**, 849–863. On the dynamics of flexible beams under large overall motions—the plane case: Parts I, II.
2. J. C. SIMO AND L. VU-QUOC 1987 *Journal of Sound and Vibration* **119**, 487–508. The role of non-linear theories in transient dynamic analysis of flexible structures.
3. J. L. MEEK AND LIU HUA 1995 *Computers and Structures* **56**, 1–14. Nonlinear dynamics analysis of flexible beams under large overall motions and the flexible manipulator simulation.
4. B. FALLAHI AND S. H.-Y. LAI 1994 *Computes and Structures* **50**, 749–755. An improved numerical scheme for characterizing dynamic behavior of high-speed rotating elastic beam structures.
5. T. R. KANE, R. R. RYAN AND A. K. BANERJEE 1987 *Journal of Guidance, Control, and Dynamics* **10**, 139–151. Dynamics of cantilever beam attached to a moving base.
6. W. J. HAERING, R. R. RYAN AND R. A. SCOTT 1994 *Journal of Guidance, Control, and Dynamics* **17**, 76–83. New formulation for flexible beams undergoing large overall plane motion.
7. M. IURA AND S. N. ATLURI 1995 *Computers and Structures* **55**, 453–462. Dynamic analysis of planar flexible beams with finite rotations by using inertial and rotating frames.
8. INNA SHARF 1995 *Journal of Guidance, Control, and Dynamics* **18**, 882–890. Geometric stiffening in multibody dynamics formulations.
9. H. YAMAURA AND K. ONO 1989 JSME *International Journal, Series III* **32**, 394–399. Nonlinear bending vibration of a rapidly driven flexible arm.
10. A. A. SHABANA AND R. SCHWERTASSEK 1998 *International Journal for Non-Linear Mechanics* **33**, 417–432. Equivalence of the floating frame of reference approach and finite element formulations.
11. C. I. CHEN, V. H. MUCINO AND C. C. SPYRAKOS 1994 *Journal of Sound and Vibration* **178**, 591–605. Flexible rotating beam: comparative modelling of isotropic and composite material including geometric non-linearity.
12. S. PUTTER AND H. MANOR 1978 *Journal of Sound and Vibration* **56**, 175–185. Natural frequencies of radial rotating beams.
13. A. YIGIT, R. A. SCOTT AND A. GALIP ULSOY 1988 *Journal of Sound and Vibration* **121**, 201–210. Flexural motion of a radially rotating beam attached to a rigid body.
14. A. KRISHNAN AND Y. J. SURESH 1998 *Computers and Structures* **68**, 473–489. A simple cubic linear element for static and free vibration analyses of curved beams.
15. H. STOLARSKI AND T. BELYTSCHKO 1982 *Journal of Applied Mechanics* **49**, 172–176. Membrane locking and reduced integration for curved elements.
16. J. T. S. WANG AND O. MAHRENHOLTZ 1975 *Ingenieur-Archiv* **44**, 399–407. Bending frequencies of a rotating curved beam.
17. D. H. HODGES, XIAOYANG SHANG AND C. E. S. CESNIK 1996 *Journal of the American Helicopter Society* 313–321. Finite element solution of nonlinear intrinsic equations for curved composite beams.

18. G. R. HEPPLER AND J. S. HANSEN 1988 *AIAA Journal* **26**, 1378–1386. Timoshenko beam finite elements using Trigonometric basis functions.
19. H. STOLARSKI AND T. BELYTSCHKO 1983 *Computer Methods in Applied Mechanics and Engineering* **41**, 279–296. Shear and membrane locking in curved C^0 elements.
20. D. B. ROBERT 1979 *Formulas for Natural Frequency and Mode Shape*. New York: Van Nostrand Reinhold.